Photoacoustics 4 (2016) 36–42

Contents lists available at ScienceDirect

Photoacoustics

journal homepage: www.elsevier.com/locate/pacs

High resolution ultrasound and photoacoustic imaging of single cells

Eric M. Strohm[a,b,c], Michael J. Moore[a,b,c], Michael C. Kolios[a,b,c,*]

[a] Department of Physics, Ryerson University, Toronto, Ontario M5B2K3, Canada
[b] Institute for Biomedical Engineering, Science and Technology (iBEST), a partnership between Ryerson University and St. Michael's Hospital, Toronto, Ontario, M5B1T8, Canada
[c] Keenan Research Centre for Biomedical Science of St. Michael's Hospital, Toronto, Ontario, M5B1T8, Canada

ARTICLE INFO

Article history:
Received 17 September 2015
Received in revised form 2 December 2015
Accepted 8 January 2016
Available online 18 January 2016

Keywords:
Acoustic microscopy
Photoacoustic microscopy
Blood smear
Leukocytes

ABSTRACT

High resolution ultrasound and photoacoustic images of stained neutrophils, lymphocytes and monocytes from a blood smear were acquired using a combined acoustic/photoacoustic microscope. Photoacoustic images were created using a pulsed 532 nm laser that was coupled to a single mode fiber to produce output wavelengths from 532 nm to 620 nm via stimulated Raman scattering. The excitation wavelength was selected using optical filters and focused onto the sample using a 20× objective. A 1000 MHz transducer was co-aligned with the laser spot and used for ultrasound and photoacoustic images, enabling micrometer resolution with both modalities. The different cell types could be easily identified due to variations in contrast within the acoustic and photoacoustic images. This technique provides a new way of probing leukocyte structure with potential applications towards detecting cellular abnormalities and diseased cells at the single cell level.

1. Introduction

Scanning acoustic microscopy (SAM) was first developed in the early 1970's at Stanford University. When using frequencies at 1000 MHz, the ultrasound imaging resolution approaches 1 μm; various biomedical applications including the imaging of single cells became readily apparent [1,2]. In SAM, the image contrast depends on the biomechanical properties of the cell assessed through the scattering and attenuation of the acoustic waves [3]. This enables high resolution images of single cells and cellular organelles with contrast not possible using optical microscopy [4–12].

Photoacoustic microscopy (PAM) uses similar hardware as acoustic microscopy, but with the addition of a pulsed laser to create the photoacoustic waves. In PAM, chromophores within the cell absorb the incident laser energy and emit an acoustic wave [13]. The acoustic wave, called a photoacoustic wave, is then detected by the same ultrasound transducer that is used in SAM. PAM is well suited to creating images of single cells using their natural endogenous chromophores, which include hemoglobin in erythrocytes [14–17], melanin in melanoma cells [14,18], DNA in cell nuclei [19] and cytochrome C in the mitochondria [17,20]. Photoacoustic images of single cells can also be created using exogenous chromophores such as dyes or nanoparticles [16,21].

Optical-resolution photoacoustic microscopy (OR-PAM) provides sub-micrometer lateral resolution, which is achieved by focusing the laser to a diffraction limited spot (approximately 200 nm using a 532 nm laser) [14,22]. The emitted photoacoustic waves are then detected using an ultrasound transducer with central frequencies up to about 100 MHz [17,23–25]. The diffraction limited laser spot provides excellent lateral resolution as photoacoustic waves are generated from within the focal spot only, however axial resolution suffers as it depends on the acoustic bandwidth of the transducer. Transducers used in these studies typically have lateral and axial resolutions in the 20–50 μm range [26], and thus are unsuitable for acoustical imaging of single cells.

We have pioneered the use of PAM using frequencies at 1000 MHz [27–29]. Combined with traditional pulse-echo acoustic microscopy, our system is capable of either acoustic or photoacoustic imaging with micrometer resolution. Images with excellent lateral and axial resolution are obtained; a quantitative analysis of the signals can also be performed to extract biomechanical or structural information about the cell [18,30–35]. To date, combined acoustic and photoacoustic imaging of the same structures at 1000 MHz has not been demonstrated. Here we demonstrate the combined imaging approach on single cells in a blood smear.

A blood smear is a monolayer of blood cells fixed and stained on top of a glass substrate [36]. The smear is composed of erythrocytes and leukocytes that are spatially separated, and as a result are ideal for both acoustic and photoacoustic microscopy. Blood smears are routinely examined by hematologists using optical microcopy to identify and diagnose blood disorders [37]. However leukocytes

* Corresponding author.
E-mail address: mkolios@ryerson.ca (M.C. Kolios).

http://dx.doi.org/10.1016/j.pacs.2016.01.001

are transparent in the visible spectrum, and difficult to identify without the use of a colorimetric stain. Metachromatic Romanowksy type dyes such as the Wright stain differentially stain cellular organelles and are often used for visual identification [38]. However, even when stained it can be difficult to identify abnormalities present in the blood cells.

Using a photoacoustic microscope outfitted with a fiber-coupled pulsed laser and a 1000 MHz transducer, this study demonstrates combined ultrasound and photoacoustic images of stained leukocytes at optical wavelengths of 532 and 600 nm. This technique has the potential to identify blood-related abnormalities and reveal structural detail that can be difficult to assess using optical microscopy alone.

2. Method

2.1. Sample preparation

Blood smears were prepared from a fresh drop of blood extracted via fingerprick from a healthy volunteer in accordance with Ryerson University Ethics Review Board (REB #2012-210), then fixed in methanol. Staining was performed by adding 1 mL of Wright–Giemsa stain (Sigma Aldrich, USA) to the slide for one minute, then 1 mL deionized water for 2 min. The slide was then washed with deionized water to remove excess stain and left to dry before imaging.

2.2. Acoustic/photoacoustic microscope

The acoustic/photoacoustic microscope (Kibero GmBH, Germany) is an inverted optical microscope equipped with a pulsed 532 nm laser (Teem Photonics, France) and an ultrasound transducer positioned above the sample. The sample was placed on the microscope translation stage where the microscope optics were used to view the sample and focus the laser, and the ultrasound transducer positioned above the sample was used to record the ultrasound and photoacoustic signals (Fig. 1A). The focal spots of the ultrasound transducer and laser were co-aligned, and crosshairs on the optical view provided by a CCD camera enable targeting of specific cells (Fig. 1B). Images were acquired by raster scanning the stage and recording the acoustic and photoacoustic signals. A schematic demonstrating photoacoustic waves emitted from a single cell is shown in Fig. 1C.

A pulsed 532 nm laser was coupled to a 2 m long single mode fiber and the collimated output was directed into the optical path of the microscope. Through cascaded stimulated Raman scattering (SRS) within the fiber, additional output wavelengths between 532 and 620 nm were observed as shown in Fig. 2A [39–42]. Adding a fiber to an existing laser setup is an inexpensive method for increasing the range of wavelengths available for photoacoustic signal generation. Using this technique, fiber-coupled 532 nm lasers with wavelength output up to 800 nm have been demonstrated [41]. Alternative methods of multispectral photoacoustic imaging use multiple dye or diode lasers, or a tunable optical parametric oscillator (OPO) laser; however, these devices are expensive. The absorption spectrum of the Wright–Giemsa stain is shown in Fig. 2B, and was measured using a UV-3600 spectrophotometer (Himadzu, Japan). Two laser wavelengths were used to probe the samples, 532 and 600 nm; the desired wavelength was selected by using optical bandpass filters (Olympus, Japan). Output energies at the selected wavelengths ranged from 1 to 5 nJ/pulse, resulting in a laser fluence between 30 and 160 mJ/cm^2 using a 1 μm diameter focal spot. The fiber-coupled laser was focused by a 20× objective (0.45 numerical aperture) onto the sample, and was co-aligned with the 1000 MHz center frequency transducer. Using these frequencies and optical focusing components, the resolution was estimated to be about 1 μm for both ultrasound and photoacoustic imaging [24,43].

Acoustic images were performed first, followed by photoacoustic imaging at 532 nm, then at 600 nm. Raster scans approximately 20 × 20 μm were made using a 0.33 μm step size, and all signals were averaged 100 times to increase the signal–noise ratio (SNR). All signals were amplified by a 40 dB low noise amplifier (Miteq, USA) and digitized at 8 GS/s (Acqiris, USA). Images were created by normalizing the acoustic and photoacoustic signals to a 256 greyscale value, with white being the strongest signal, and black the lowest. Composite photoacoustic images combining the 532 and 600 nm scans were made by assigning the 532 nm image a green channel, the 600 nm a red channel and then merging the images. Further details on the acoustic and photoacoustic methods can be found in [18,30,35].

3. Results

The ultra-high frequency acoustic/photoacoustic microscope (UHF–APAM) is a hybrid of optical resolution (OR–PAM) and acoustic resolution (AR–PAM) photoacoustic microscopy. Using ultrasound and photoacoustic frequencies at 1000 MHz, this system is capable of micrometer-resolution imaging with high sensitivity. This enhanced photoacoustic sensitivity is achieved as the photoacoustic signal generated at the micrometer laser spot is amplified by the geometrical gain of the focused ultrasound

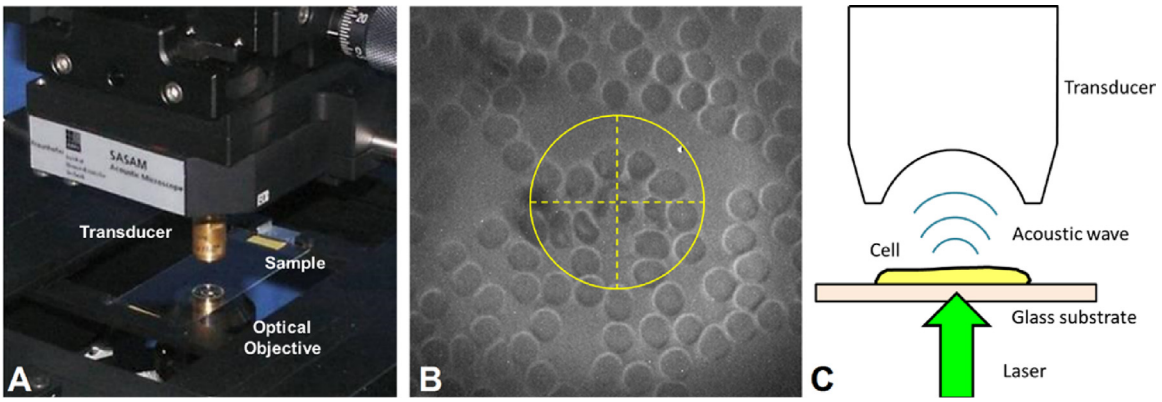

Fig. 1. The acoustic microscope: (A) the transducer is positioned above the sample slide, and the optics below are used to focus the laser and to view the sample. (B) An optical view of a stained blood smear with the transducer in place, the crosshairs are used to target each cell. A neutrophil is visible within the crosshairs. (C) A schematic showing photoacoustic waves generated from a cell on top of a glass slide travelling towards the transducer.

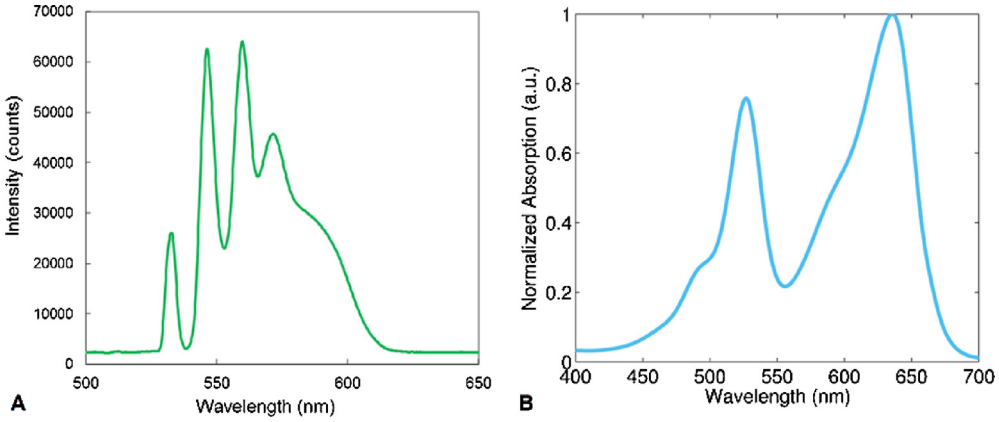

Fig. 2. (A) The optical wavelengths emitted from the 532 nm fiber-coupled laser. Additional emission peaks at wavelengths greater than 532 nm occur due to stimulated Raman Scattering within the fiber. (B) The absorption spectrum of the Wright–Giemsa stain.

transducer. Micrometer-sized objects emit waves with significant signal energy content near GHz frequencies [34,44,45] and the wide transducer bandwidth (600 MHz) allows for micrometer-scale axial resolution [18].

The Wright–Giemsa stain is a mixture of several dyes commonly used to stain blood smears. The constituent dyes are selectively absorbed in various organelles, resulting in pink, red, blue and purple hues. Stained leukocytes were imaged first with ultrasound, and subsequently with photoacoustics using optical wavelengths of 532 and 600 nm. Acquired optical, ultrasound and photoacoustic images of the most abundant leukocytes in blood – neutrophils, lymphocytes, and monocytes – are shown in Figs. 3–5 , respectively.

3.1. Neutrophils

In neutrophils, the cytoplasm was stained light pink and the nuclear lobes were stained blue (Fig. 3). The areas of strongest acoustic attenuation generally coincided with the location of the nucleus; however, areas of increased attenuation outside of the stained nuclear area were sometimes also observed (center of cell, Fig. 3F). In all cases, acoustic attenuation through the neutrophil was less than attenuation through the surrounding red blood cells. Strong photoacoustic signals were obtained from the nucleus at both 532 and 600 nm, with negligible signal from the cytoplasm. Weak photoacoustic signals were detected in areas surrounding the nucleus at 532 nm which were not present in the 600 nm image (Fig. 3C and G).

3.2. Lymphocytes

In lymphocytes, the nucleus stains dark purple while the cytoplasm is colored light blue (Fig. 4). The nucleus of lymphocytes generally occupies most of the cell volume. Unlike the neutrophil, the acoustic attenuation of the lymphocyte nucleus was less than that of the cytoplasm. The photoacoustic signal from the nucleus was much stronger than the cytoplasm in the 532 nm image; interestingly, this trend was reversed at 600 nm. Structures within the nucleus (such as the dark spot in Fig. 4B that coincides with the bright spot in Fig. 4D) are not easily detectable in the optical images.

3.3. Monocytes

Stained monocytes express color profiles similar to stained lymphocytes, with dark purple nuclei and light purple cytoplasm (Fig. 5). Vacuoles are sometimes present, as they were in these cells. The acoustic attenuation of the nucleus was typically less

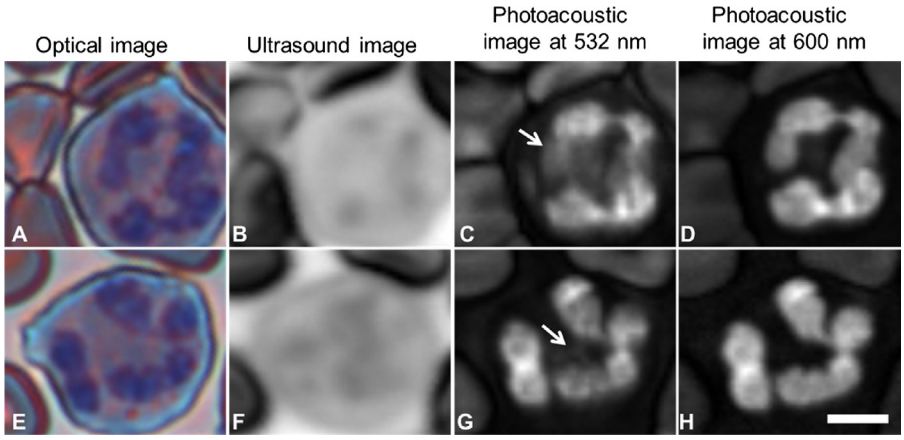

Fig. 3. Stained neutrophils: optical (A and E), ultrasound (B and F), photoacoustic at 532 nm (C and G) and photoacoustic at 600 nm (D and H) images of neutrophils. The arrows indicate photoacoutic signals from the nucleus that are visible at 532 nm, but not at 600 nm (C and G). The scale bar is 5 μm.

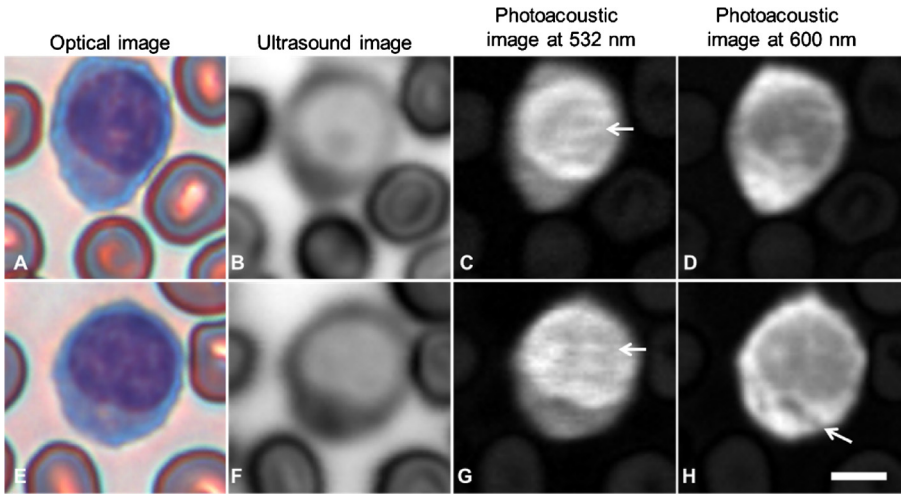

Fig. 4. Stained lymphocytes: optical (A and E), ultrasound (B and F), photoacoustic at 532 nm (C and G) and photoacoustic at 600 nm (D and H) images of lymphocytes. The arrows indicate areas of fine like structure (C and G) and voids in the signal (H) that are not observed in the optical image. The scale bar is 5 μm.

than the cytoplasm; however, the nuclear outline was not clearly defined. The photoacoustic signal from the nucleus was stronger than the cytoplasm at both 532 and 600 nm, and the signal from the cytoplasm was significantly stronger at 600 nm than at 532 nm. The vacuoles were easier to see in the photoacoustic images than the acoustic images.

3.4. Composite photoacoustic images

The composite photoacoustic images were merged using a green channel from the 532 nm image, and a red channel from the 600 nm image to accentuate features not easily seen in the grayscale images as shown in Fig. 6 (see Supplementary information for details on the method). Image areas that were predominately green indicated signals that were stronger in the 532 nm image compared to the 600 nm image, while areas that were predominately orange or red indicated signals that were stronger in the 600 nm image compared to the 532 nm image. Yellow areas indicated equal signal amplitude in both the 532 and 600 nm images. The lymphocytes showed a green nuclei, monocytes a yellow nuclei, and the neutrophils a mix of yellow, green and red. The cell types can be easily identified according to the shape and color of the cell regions.

4. Discussion

These results demonstrate that in all cases, acoustic and photoacoustic images of common leukocytes stained with a metachromatic stain can be used to identify the cell types, even for cells with principally similar color profiles such as lymphocytes and monocytes. Additional features and fine structures that are difficult to see in the stained optical images are enhanced in the photoacoustic images.

Ultrasound imaging using GHz frequencies suffers from very high attenuation, and the maximum penetration depth is a couple cell layers at most; it is ideally suited for monolayer samples such as blood smears. The acoustic attenuation within the neutrophil was stronger throughout the nuclear lobes than in the cytoplasm. This has been observed in transmission acoustic microscopy studies of leukocytes, where the nucleus of fixed and stained neutrophils was more attenuating than the cytoplasm [46]. The nucleus of live unstained MCF-7 breast cancer cells was also found

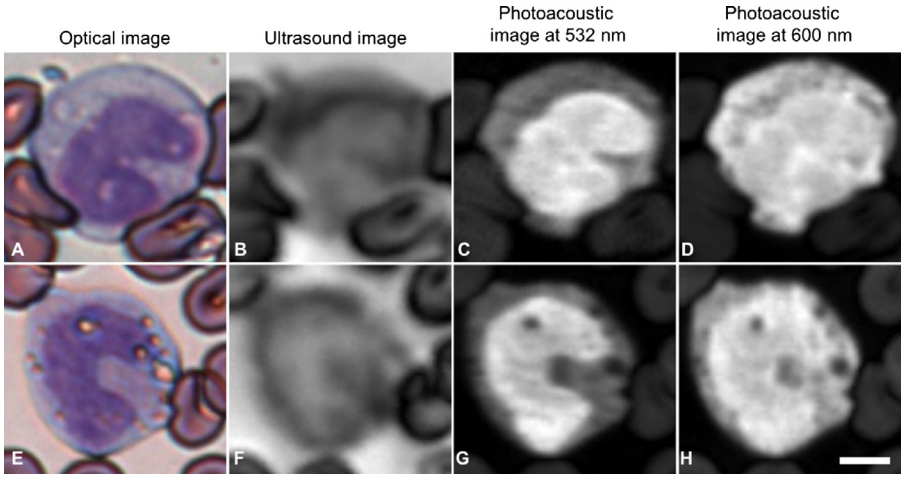

Fig. 5. Stained monocytes: optical (A and E), ultrasound (B and F), photoacoustic at 532 nm (C and G) and photoacoustic at 600 nm (D and H) images of monocytes. The scale bar is 5 μm.

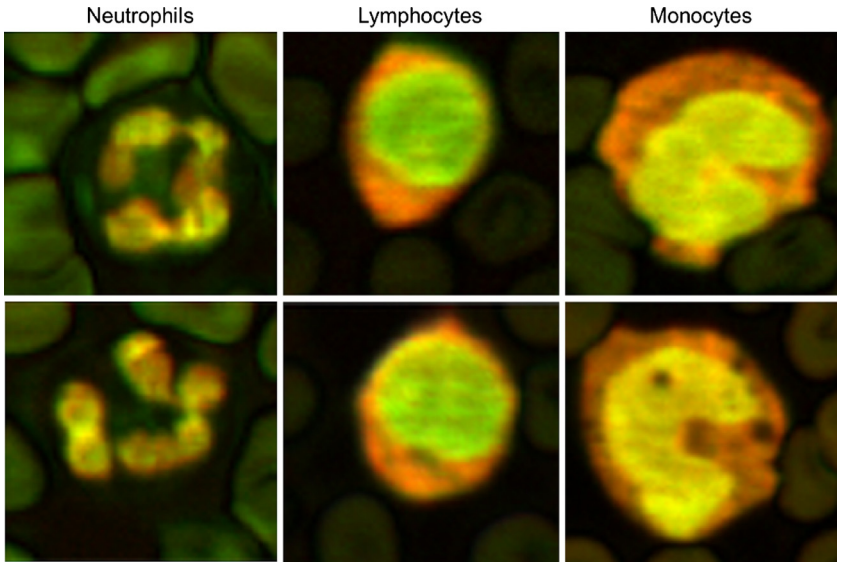

Fig. 6. Composite photoacoustic images of the neutrophils, lymphocytes and monocytes created by merging the 532 nm and 600 nm photoacoustic images from figures 2–5. The color provides additional metrics that can be used to differentiate the cell types.

to be more attenuating than the cytoplasm [30]. However for the lymphocytes and monocytes, the opposite trend was observed; the nucleus was less attenuating than the cytoplasm. The chromatin in the nuclei of neutrophils is highly condensed [47], which may be why the attenuation is higher in these cells versus the other leukocytes.

A chromophore with strong optical absorption is required for photoacoustic wave generation, with the amplitude of the generated wave generally being proportional to the absorption cross section of the chromophore and the number of chromophore molecules per unit volume [13]. While there are potential structures in cells that absorb within the visible wavelength range, such as cytochromes [20], photoacoustic signals from unstained leukocytes were not detected at 532 nm, even when using increased laser energies up to 100 nJ per pulse. Thus, the photoacoustic signals depend entirely on the staining properties of the cell. Due to the differential staining, the photoacoustic contrast between the nucleus and cytoplasm is very high and features in the photoacoustic images not readily visible in the optical images become apparent. This includes the faint photoacoustic signals around the nuclear lobes in the neutrophils (Fig. 3C and G), the fine line-like structures within the nucleus (Fig. 4C and G) and the void outside the nucleus (Fig. 4H) of the lymphocytes, and the irregular nuclear shape in the monocytes (Fig. 5C, D, G and H). The composite figures combine the 532 nm and 600 nm photoacoustic images to create a false color image where the cell features and the cell types can be more easily identified compared to the monochrome photoacoustic images at either 532 or 600 nm (Fig. 6). In these measurements, the photoacoustic signals from the stained leukocytes are 5–10× stronger than those from the surrounding stained erythrocytes, which are typically the strongest chromophore in tissues at these wavelengths and provide high contrast for photoacoustic imaging of vessels and blood-rich structures [48–50].

In this proof of concept study, healthy leukocytes were examined using the Wright–Giemsa stain which is the gold standard for examining blood smears. Hematologists typically observe many cell features to identify abnormalities, such as the coarseness of the chromatin, sub-micrometer defects and nuclear shape/morphology to make a diagnosis [51]. These abnormal features may affect the ultrasound and photoacoustic images; the enhanced contrast provided suggests abnormal leukocytes may be easier to identify using this combined acoustic–photoacoustic method compared to optical observation. Differences in the acquired photoacoustic images can be used to identify leukocytes with similar staining profiles but with inclusions that may not be visible using optical microscopy, particularly when using additional dyes that have different absorption wavelengths that are targeted towards detecting specific cell features, such as using Sudan Black B for staining granules and Auer rods, or new methylene blue for staining reticulocytes [37].

The lateral resolution of both the acoustic and photoacoustic images was estimated to be about 1 μm, which approaches the resolution limit obtainable using traditional optical microscopy [52]. Photoacoustic imaging using a diffraction limited resolution (200 nm when using an optical wavelength of 532 nm) is possible when using highly focused objectives [14]; the resolution can be further enhanced past the diffraction limit to $<$100 nm by exploiting non-linear photoacoustic effects [17]. At these resolutions, it may be possible to image single granules present in cells, and resolve fine structures and inclusions that are not possible to see optically, particularly when a multi-spectral approach is used. Future work will concentrate on improving the resolution of our hybrid system, probing diseased blood cells, and investigating the use of combinations of different optical wavelengths with different dyes as well as label-free methods that may be used to enhance the contrast and resolution for identifying abnormal cells.

5. Conclusion

This study is the first demonstration of combined ultrasound and photoacoustic measurements of single leukocytes with micrometer resolution. Stained neutrophils, lymphocytes and monocytes exhibited variations in the acoustic images that generally coincided with the nuclear structure. The photoacoustic images generated using optical wavelengths at 532 nm and 600 nm showed striking detail that could not be observed in optical microscopy. This combined imaging method could be used to help diagnose disease, and detect small defects that cannot be seen using traditional optical microscopy.

Conflict of interest

The authors have a financial interest in Echofos Medical, which, however, did not support this work.

Acknowledgements

This research was undertaken, in part, thanks to funding from The Canadian Cancer Society generously supported by the Lotte & John Hecht Memorial Foundation (#702161), the Natural Sciences and Engineering Research Council of Canada, and the Canada Research Chairs Program. Funding to purchase the equipment was provided by the Canada Foundation for Innovation, the Ontario Ministry of Research and Innovation, and Ryerson University.

Appendix A. Supplementary data

Supplementary data associated with this article can be found, in the online version, at http://dx.doi.org/10.1016/j.pacs.2016.01.001.

References

[1] R.A. Lemons, C.F. Quate, A scanning acoustic microscope, IEEE Ultrasonics Symposium (1973) 18–21, doi:http://dx.doi.org/10.1109/ULTSYM.1973.196138.
[2] R.A. Lemons, C.F. Quate, Acoustic microscope—scanning version, Appl. Phys. Lett. 24 (1974) 163.
[3] A. Briggs, O. Kolosov, Acoustic Microscopy, Oxford University Press, USA, 2009.
[4] H.K. Wickramasinghe, M. Hall, Phase imaging with the scanning acoustic microscope, Electron. Lett. 12 (1976) 637.
[5] R.N. Johnston, A. Atalar, J. Heiserman, V. Jipson, C.F. Quate, Acoustic microscopy: resolution of subcellular detail, Proc. Natl. Acad. Sci. 76 (1979) 3325–3329.
[6] D. Rugar, J. Heiserman, S. Minden, C.F. Quate, Acoustic microscopy of human metaphase chromosomes, J. Microsc. 120 (1980) 193–199.
[7] R.A. Lemons, C.F. Quate, Advances in mechanically scanned acoustic microscopy, Ultrasonics Symposium 1974 (1974) 41–44.
[8] E.A. Schenk, R.W. Waag, A.B. Schenk, J.P. Aubuchon, Acoustic microscopy of red blood cells, J. Histochem. Cytochem. 36 (1988) 1341–1351.
[9] C.F. Quate, A. Atalar, H.K. Wickramasinghe, Acoustic microscopy with mechanical scanning—a review, Proceedings of the IEEE vol. 67 (1979) 1092–1114.
[10] J. Litniewski, J. Bereiter-Hahn, Measurements of cells in culture by scanning acoustic microscopy, J. Microsc. 158 (1990) 95–107.
[11] H. Lüers, K. Hillmann, J. Litniewski, J. Bereiter-Hahn, Acoustic microscopy of cultured cells, Cell Biochem. Biophys. 18 (1991) 279–293.
[12] A. Briggs, W. Arnold, Advances in Acoustic Microscopy, Plenum Pub. Corp., 1996.
[13] M. Xu, L.V. Wang, Photoacoustic imaging in biomedicine, Rev. Sci. Instrum. 77 (2006) 041101–041101–22.
[14] C. Zhang, K. Maslov, L.V. Wang, Subwavelength-resolution label-free photoacoustic microscopy of optical absorption in vivo, Opt. Lett. 35 (2010) 3195–3197.
[15] K. Maslov, H.F. Zhang, S. Hu, L.V. Wang, Optical-resolution confocal photoacoustic microscopy, Proceedings of SPIE vol. 6856 (2008) 68561I–68561I–7.
[16] B. Rao, K. Maslov, A. Danielli, R. Chen, K.K. Shung, Q. Zhou, et al., Real-time four-dimensional optical-resolution photoacoustic microscopy with Au-nanoparticle assisted sub-diffraction-limit resolution, Opt. Lett. 36 (2011) 1137–1139.
[17] A. Danielli, K. Maslov, A. Garcia-Uribe, A.M. Winkler, C. Li, L. Wang, et al., Label-free photoacoustic nanoscopy, J. Biomed. Opt. 19 (2014) 086006–086006.
[18] E.M. Strohm, E.S.L. Berndl, M.C. Kolios, High frequency label-free photoacoustic microscopy of single cells, Photoacoustics 1 (2013) 49–53.
[19] D.-K. Yao, K. Maslov, K.K. Shung, Q. Zhou, L.V. Wang, In vivo label-free photoacoustic microscopy of cell nuclei by excitation of DNA and RNA, Opt. Lett. 35 (2010) 4139–4141.
[20] C. Zhang, Y.S. Zhang, D.-K. Yao, Y. Xia, L.V. Wang, Label-free photoacoustic microscopy of cytochromes, J. Biomed. Opt. 18 (2013) 020504–020504.
[21] Y. Zhang, X. Cai, Y. Wang, C. Zhang, L. Li, S.-W. Choi, et al., Non-invasive photoacoustic microscopy of living cells in two and three dimensions through enhancement by a metabolite dye, Angew. Chem. Int. Ed. Engl. 50 (2011) 7359–7363.
[22] C. Zhang, K. Maslov, S. Hu, R. Chen, Q. Zhou, K.K. Shung, et al., Reflection-mode submicron-resolution in vivo photoacoustic microscopy, J. Biomed. Opt. 17 (2012) 020501–020501–4.
[23] J. Yao, L.V. Wang, Sensitivity of photoacoustic microscopy, Photoacoustics 2 (2014) 87–101.
[24] J. Yao, L.V. Wang, Photoacoustic microscopy, Laser Photonics Rev. 7 (2013) 758–778.
[25] L.V. Wang, Multiscale photoacoustic microscopy and computed tomography, Nat. Photonics 3 (2009) 503–509.
[26] C.R. Hill, J.C. Bamber, G. Haar, Physical Principles of Medical Ultrasonics, John Wiley and Sons, Hoboken, New Jersey, 2004.
[27] W. Bost, F. Stracke, E.C. Weiss, S. Narasimhan, M.C. Kolios, R. Lemor, High frequency optoacoustic microscopy, Annual International Conference of the IEEE Engineering in Medicine and Biology Society (2009) 5883–5886.
[28] M. Rui, S. Narashimhan, W. Bost, F. Stracke, E. Weiss, R. Lemor, et al., Gigahertz optoacoustic imaging for cellular imaging, Proceedings of SPIE vol. 7564 (2010) 756411–756411–6.
[29] M. Rui, W. Bost, E.C. Weiss, R. Lemor, M.C. Kolios, Photoacoustic microscopy and spectroscopy of individual red blood cells, Int. J. Radiat. Oncol. Biol. Phys. (2010) 3–5.
[30] E.M. Strohm, G.J. Czarnota, M.C. Kolios, Quantitative measurements of apoptotic cell properties using acoustic microscopy, IEEE Transactions on Ultrasonics, Ferroelectrics and Frequency Control 57 (2010) 2293–2304.
[31] M.C. Kolios, E.M. Strohm, G.J. Czarnota, Acoustic microscopy of cells, in: J. Mamou, M.L. Oelze (Eds.), Quantitative Ultrasound in Soft Tissues, Springer, Netherlands, 2013, pp. 315–341.
[32] E.M. Strohm, M.C. Kolios, Classification of blood cells and tumor cells using label-free ultrasound and photoacoustics, Cytometry 87 (2015) 741–749.
[33] M.N. Fadhel, E.S.L. Berndl, E.M. Strohm, M.C. Kolios, High-frequency acoustic impedance imaging of cancer cells, Ultrasound Med. Biol. 41 (2015) 2700–2713.
[34] E.M. Strohm, I. Gorelikov, N. Matsuura, M.C. Kolios, Modeling photoacoustic spectral features of micron-sized particles, Phys. Med. Biol. 59 (2014) 5795–5810.
[35] E.M. Strohm, Elizabeth S.L. Berndl, M.C. Kolios, Probing red blood cell morphology using high frequency photoacoustics, Biophys. J. 105 (2013) 59–67.
[36] M.M. Wintrobe, J.P. Greer, G.R. Lee, Wintrobe's Clinical Hematology, Wolters Kluwer/Lippincott Williams & Wilkins, Philadelphia, 2009.
[37] B.J. Bain, Blood Cells: A Practical Guide, 4th ed., Wiley-Blackwell, 2006.
[38] R.W. Horobin, K.J. Walter, Understanding Romanowsky staining. I: the Romanowsky–Giemsa effect in blood smears, Histochemistry 86 (1987) 331–336.
[39] A.K. Loya, J.P. Dumas, T. Buma, Photoacoustic microscopy with a tunable source based on cascaded stimulated Raman scattering in a large-mode area photonic crystal fiber, IEEE Ultrasonics Symposium (2012) 1208–1211.
[40] P. Hajireza, A. Forbrich, R.J. Zemp, Multifocus optical-resolution photoacoustic microscopy using stimulated Raman scattering and chromatic aberration, Opt. Lett. 38 (2013) 2711.
[41] P. Hajireza, A. Forbrich, R. Zemp, In-vivo functional optical-resolution photoacoustic microscopy with stimulated Raman scattering fiber-laser source, Biomed. Opt. Express 5 (2014) 539–546.
[42] T. Buma, B.C. Wilkinson, T.C. Sheehan, Near-infrared spectroscopic photoacoustic microscopy using a multi-color fiber laser source, Biomed. Opt. Express 6 (2015) 2819.
[43] R. Weglein, R. Wilson, Image resolution of the scanning acoustic microscope, Appl. Phys. Lett. (1977) 117–120.
[44] G.J. Diebold, M.I. Khan, S.M. Park, Photoacoustic "signatures" of particulate matter: optical production of acoustic monopole radiation, Science 250 (1990) 101–104.
[45] G.J. Diebold, T. Sun, M.I. Khan, Photoacoustic monopole radiation in one, two, and three dimensions, Phys. Rev. Lett. 67 (1991) 3384–3387.
[46] R. Lemons, C. Quate, Acoustic microscopy: biomedical applications, Science 188 (1975) 905–911.
[47] B. Young, J.W. Heath, A. Stevens, J.S. Lowe, P.R. Wheater, H.G. Burkitt, Wheater's Functional Histology: A Text and Colour Atlas, Churchill Livingstone, Edinburgh, New York, 2000.
[48] X. Wang, Y. Pang, G. Ku, X. Xie, G. Stoica, L.V. Wang, Noninvasive laser-induced photoacoustic tomography for structural and functional in vivo imaging of the brain, Nat. Biotechnol. 21 (2003) 803–806.
[49] H.F. Zhang, K. Maslov, G. Stoica, L.V. Wang, Functional photoacoustic microscopy for high-resolution and noninvasive in vivo imaging, Nat. Biotechnol. 24 (2006) 848–851.
[50] L.V. Wang, S. Hu, Photoacoustic tomography: in vivo imaging from organelles to organs, Science 335 (2012) 1458–1462.
[51] B.F. Rodak, G.A. Fritsma, E. Keohane, Hematology: Clinical Principles and Applications, Elsevier Health Sciences, 2007.
[52] M. Spencer, Fundamentals of Light Microscopy, CUP Archive, 1982.

Eric M. Strohm received his B.Sc. degree in Physics from McMaster University in 1999. From 2002–2007, he was employed as a member of research staff at the Xerox Research Centre of Canada. He received his M.Sc. degree in 2009 and Ph.D. degree in 2013 in Biomedical Physics from Ryerson University. He is currently a Postdoctoral Fellow in the Biomedical Ultrasound Laboratory at Ryerson University. His research interests include ultrasound and photoacoustic imaging and spectroscopy, photonics, nanotechnology, and microfluidics for the characterization of biological cells and tissues.

Michael J. Moore received his B. Math degree in Mathematical Physics from the University of Waterloo, Ontario, Canada, in 2013. He is currently pursuing his Ph.D. degree at Ryerson University, Ontario, Canada, in the CAMPEP Accredited

Biomedical Physics program. His research interests include acoustic microscopy, photoacoustic microscopy, and high-frequency quantitative photoacoustics of single biological cells.

Michael C. Kolios is a Professor in the Department of Physics at Ryerson University and associate Dean of Research and Graduate Studies in the Faculty of Science. His work focuses on the use of ultrasound and optics in the biomedical sciences. He has published 73 peer-reviewed journal publications, 5 book chapters, and 96 papers in conference proceedings. He has been invited to speak at 35 different organizations or conferences, and has been the keynote and plenary speaker for conferences in Canada, India and China. He has received numerous teaching and research awards, including the Canada Research Chair in Biomedical Applications of Ultrasound and the Ontario Premier's Research Excellence Award. He is on the editorial board of the journals Ultrasound Imaging and Photoacoustics and is member of many national and international committees, including the IEEE International Ultrasonics Symposium Technical Program Committee. He is a member of the National Institutes of Health (NIH) Biomedical Imaging Technology A study section and was previously a member of the Canadian Institutes of Health Research (CIHR) Medical Physics and Imaging (MPI) panel.